Quarterly Journal of the
Royal Meteorological Society

Analysis sensitivity calculation within an Ensemble Kalman filter

Journal:	*Quarterly Journal of the Royal Meteorological Society*
Manuscript ID:	QJ-08-0083.R1
Wiley - Manuscript type:	Research Article
Date Submitted by the Author:	
Complete List of Authors:	Liu, Junjie; University of Maryland, Atmospheric and Oceanic Science Kalnay, Eugenia; University of Maryland, Atmospheric and Oceanic Science Miyoshi, Takemasa; University of Maryland, Atmospheric and Oceanic Science Cardinali, Carla; ECMWF
Keywords:	Analysis sensitivity, Ensemble Kalman filter, Cross Validation

scholarONE™
Manuscript Central

Analysis sensitivity calculation in Ensemble Kalman Filter

Junjie Liu[1], Eugenia Kalnay[2], Takemasa Miyoshi[2], and Carla Cardinali[3]

[1]University of California, Berkeley, CA, USA
[2]University of Maryland, College Park, MD, USA
[3]ECMWF, Data Assimilation Section, Reading, UK

For Peer Review

Abstract

Analysis sensitivity indicates the sensitivity of analysis to observations, which is complementary to the sensitivity of the analysis to background. Following Cardinali et al. (2004), this paper discussed a method to calculate this quantity in Ensemble Kalman Filter without approximations. The calculation procedure and the geometrical interpretation showing that analysis sensitivity is proportional to analysis error and anti-correlated with observation error are experimentally verified with the Lorenz-40 variable model. Cross-validation in its original formulation (Wahba, 1990) is computationally unfeasible even for a model with a moderate number of degrees of freedom, but is computed efficiently using analysis sensitivity in an EnKF.

Idealized experiments based on a simplified-parameterization primitive equation global model show that information content (trace of analysis sensitivity of any subset of observations) agrees qualitatively with the actual observation impact calculated from much more expensive data denial experiments, not only for the same type of dynamical variable, but also for different types of dynamical variables.

For Peer Review

1. Introduction

Observations are the central information introduced into numerical weather prediction system through data assimilation; a process that combines observations with background forecasts based on their error statistics. With the increase of observation datasets assimilated in modern data assimilation systems, such as the assimilation of Advanced InfraRed Satellite (AIRS) and the Infrared Atmospheric Sounding Interferometer (IASI), it is important to examine questions such as how much information content a new observation dataset has, what is the spatial distribution of the impact of the new observations on the analysis, and what is the relative influence of background forecasts and observations on the analyses.

The computation of analysis sensitivity (also called as self-sensitivity), a quantity introduced by Cardinali et al. (2004) can address these questions. The larger the analysis sensitivity is, the larger is the influence of observations, and the smaller the influence of background forecasts. Since analysis sensitivity is a function of the analysis error covariance that is not explicitly calculated in variational data assimilation schemes, Cardinali et al. (2004) proposed an approximate method to calculate this quantity within a 4D-Var data assimilation framework. They showed that the trace of analysis sensitivity of a particular observation data type represented the information content of that type of observations, and the relative importance of different observation types determined by information content was in good qualitative agreement with the observation impact from other studies. In addition, information content has also been used in channel selection in multi-thousand channel satellite instruments, such as in IASI (Rabier et al., 2002).

For Peer Review

Though the approximate method to calculate analysis sensitivity within 4D-Var is computationally possible, it introduces spurious values that are not within the theoretical value range (between 0 and 1). In contrast with variational data assimilation schemes, Ensemble Kalman filters (EnKF) (Evensen, 1994; Anderson, 2001; Bishop et al., 2001; Houtekamer and Mitchell, 2001; Whitaker and Hamill, 2002; Ott et al., 2004; Hunt et al., 2007) generate ensemble analyses that can be used to calculate the analysis error covariance. Because of this characteristic, it would be more straightforward to calculate analysis sensitivity in EnKF than in variational data assimilation. In addition, the Cross Validation (CV) (Wahba, 1990) score can be exactly calculated in EnKF based on the analysis sensitivity, observation and analysis values without carrying out data denial experiments (section 4). In the variational formulation, because of the approximations made in calculating analysis sensitivities, cross-validation cannot be exactly computed. In this paper, we follow Cardinali et al. (2004), show how to calculate analysis sensitivity and the related diagnostics in EnKF, and further study the properties and possible applications of these diagnostics. This paper is organized as follows: section 2 describes how to calculate analysis sensitivity in EnKF. In section 3, with a geometrical interpretation method adapted from Desroziers et al. (2005), we show that analysis sensitivity is proportional to the analysis errors and anti-correlated with the observation errors. With the Lorenz-40 variable model (Lorenz and Emanuel, 1998), section 4 verifies the self-sensitivity calculation procedure, and shows the squared analysis value change based on analysis sensitivity can differentiate abnormal observations from normal ones. In addition, the geometrical interpretation is experimentally tested in this section. In section 5, with a primitive equation model and a perfect model experimental setup (no

For Peer Review

model error), we examine the effectiveness of the trace of self-sensitivity in assessing the observation impact obtained from data denial experiments. Section 6 contains a summary and conclusions.

2. Calculation of analysis sensitivity in EnKF

In this section, we first briefly derive the analysis sensitivity valid for all data assimilation schemes (equations (1), (2), (3), equivalent to equations (3.1), (3.4), and (3.5) in Cardinali et al., 2004) and then focus on how to calculate this quantity in EnKF.

In data assimilation, the analysis state $\mathbf{x}^a$ combines the background (an n-dimensional vector $\mathbf{x}^b$) and the observations (a p-dimensional vector $\mathbf{y}^o$) based on a weighting matrix $\mathbf{K}$, which can be expressed as:

$$\mathbf{x}^a = \mathbf{K}\mathbf{y}^o + (\mathbf{I}_n - \mathbf{K}\mathbf{H})\mathbf{x}^b \tag{1}$$

The $(n \times p)$ gain matrix $\mathbf{K} = \mathbf{P}^b\mathbf{H}^T(\mathbf{H}\mathbf{P}^b\mathbf{H}^T + \mathbf{R})^{-1}$ weighs the error covariance of the background $\mathbf{P}^b$ and of the observations $\mathbf{R}$, and $\mathbf{H}(\bullet)$ is the linearized observation operator that transforms a perturbation from model space to observation space. From Equation (1), the analysis sensitivity with respect to observations is:

$$\mathbf{S}^o = \frac{\partial \hat{\mathbf{y}}^a}{\partial \mathbf{y}^o} = \mathbf{K}^T\mathbf{H}^T = \mathbf{R}^{-1}\mathbf{H}\mathbf{P}^a\mathbf{H}^T, \tag{2}$$

and the sensitivity with respect to background is given by

$$\mathbf{S}^b = \frac{\partial \hat{\mathbf{y}}^a}{\partial \mathbf{y}^b} = \mathbf{I}_p - \mathbf{K}^T\mathbf{H}^T = \mathbf{I}_p - \mathbf{S}^o \tag{3}$$

where $\hat{\mathbf{y}}^a = \mathbf{H}\mathbf{x}^a = \mathbf{H}\mathbf{K}\mathbf{y}^o + (\mathbf{I}_p - \mathbf{H}\mathbf{K})\mathbf{y}^b$ is the projection of analysis (equation (1)) on observation space, and $\mathbf{y}^b = \mathbf{H}\mathbf{x}^b$ is the projection of background on observation space.

For Peer Review

$\mathbf{P}^a = \mathbf{P}^b\mathbf{H}^T(\mathbf{H}\mathbf{P}^b\mathbf{H}^T + \mathbf{R})^{-1}$ is the analysis error covariance. The matrix $\mathbf{S}^o$ is called *influence matrix*, because the elements of this matrix reflect how much influence the observations have on the analysis state. The diagonal elements of the matrix $\mathbf{S}^o$ are analysis self-sensitivities, and the off-diagonal elements are cross sensitivities. Similarly $\frac{\partial \hat{\mathbf{y}}^a}{\partial \mathbf{y}^b}$ reflects how much influence the background has on the analysis. As shown in Cardinali et al. (2004), the self-sensitivity of the analysis with respect to observation and the corresponding background at that observation location are complementary (i.e., they add up to one), and self-sensitivity has no unit and its theoretical value is between 0 and 1 when the observation errors are not correlated ($\mathbf{R}$ is diagonal).

EnKF generates ensemble analyses in every analysis cycle, and the analysis error covariance can be written as products of ensemble analysis perturbations, so in EnKF equation (2) can be written as:

$$\mathbf{S}^o = \mathbf{R}^{-1}\mathbf{H}\mathbf{P}^a\mathbf{H}^T = \frac{1}{n-1}\mathbf{R}^{-1}(\mathbf{H}\mathbf{X}^a)(\mathbf{H}\mathbf{X}^a)^T \tag{4}$$

where $\mathbf{H}\mathbf{X}^a$ is the analysis ensemble perturbation matrix in the observation space whose i^{th} column is

$$\mathbf{H}\mathbf{X}^{ai} \cong h(\mathbf{x}^{ai}) - \frac{1}{n}\sum_{i=1}^{n} h(\mathbf{x}^{ai}) \tag{5}$$

$\mathbf{x}^{ai}$ is the i^{th} analysis ensemble member, n is the total number of ensemble analyses, and $h(\bullet)$ is the observation operator, which can be linear or nonlinear. When the observation operator is linear, the right hand side and the left hand side of Equation (5) are exactly equal. Otherwise, the left hand side is a linear approximation of the right hand side. When the observation errors are not correlated, the self-sensitivity can be written as:

For Peer Review

$$S^{o}_{jj} = \frac{\partial \hat{\mathbf{y}}^{a}_{j}}{\partial \mathbf{y}^{o}_{j}} = \left(\frac{1}{n-1}\right)\frac{1}{\sigma_j^2}\sum_{i=1}^{n}(\mathbf{HX}^{ai})^{T}_{j}(\mathbf{HX}^{ai})_{j} \quad (6)$$

and the cross sensitivity, which represents the change of $\hat{y}^{a}_{j}$ with respect to the variation of observation y^{o}_{l}, can be written as:

$$S^{o}_{jl} = \frac{\partial \hat{\mathbf{y}}^{a}_{j}}{\partial \mathbf{y}^{o}_{l}} = \left(\frac{1}{n-1}\right)\frac{1}{\sigma_j^2}\sum_{i=1}^{n}[(\mathbf{HX}^{ai})^{T}_{j}(\mathbf{HX}^{ai})_{l}] \quad (7)$$

where σ_j^2 is the j^{th} observation error variance. Equation (5) indicates that the calculation of the self-sensitivity and cross sensitivity in EnKF only requires applying the observation operator on each analysis ensemble member, and then doing scalar calculation based on equations (6) and (7). In section 4, this calculation procedure will be verified with the Lorenz-40 variable model. The calculation of the self-sensitivity based on equation (6) requires no approximations when the observation errors are not correlated, so that S^{o}_{jj} satisfies the theoretical value limits (between 0 and 1). In 4D-Var, by contrast, the calculation of analysis error covariance is based on a truncated eigenvector expansion with vectors obtained through the Lanczos algorithm, which can introduce spurious values larger than one (Cardinali et al., 2004).

3. Geometric interpretation of self-sensitivity

Equations (6) shows that the analysis sensitivity is proportional to the analysis error variance and inversely proportional to the observation error variance. Since in most cases, the analysis and observation error statistics used in data assimilation do represent the accuracy of analyses and observations respectively, equation (6) implicitly indicates that analysis sensitivity increases with the analysis errors and decreases with the

For Peer Review

observation errors. In this section, we adapt the geometrical interpretation that Desroziers et al. (2005) used to explain the relationship among background error, observation error and analysis error to further show this relationship in the space of eigenvectors $\mathbf{V}$ of the matrix $\mathbf{HK}$.

Following the same notation as Desroziers et al. (2005), we rewrite equation $\hat{\mathbf{y}}^a = \mathbf{HK}\mathbf{y}^o + (\mathbf{I}_p - \mathbf{HK})\mathbf{y}^b$ by subtracting $h(\mathbf{x}^t)$, the true state in observation space, from both sides and obtain

$$\hat{\mathbf{y}}^a - h(\mathbf{x}^t) = \mathbf{HK}(\mathbf{y}^o - h(\mathbf{x}^t)) + (\mathbf{I}_p - \mathbf{HK})(\mathbf{y}^b - h(\mathbf{x}^t)) \quad (8)$$

In equation (8), $\delta\hat{\mathbf{y}}^a = \hat{\mathbf{y}}^a - h(\mathbf{x}^t)$, $\delta\mathbf{y}^b = \mathbf{y}^b - h(\mathbf{x}^t)$ and $\delta\mathbf{y}^o = \mathbf{y}^o - h(\mathbf{x}^t)$ are analysis and background errors in observation space, and observation errors respectively. Then equation (8) can be written as,

$$\delta\hat{\mathbf{y}}^a = \mathbf{HK}\delta\mathbf{y}^o + (\mathbf{I}_p - \mathbf{HK})\delta\mathbf{y}^b \quad (9)$$

Following Desroziers et al. (2005), we give a geometrical interpretation in the space of eigenvectors $\mathbf{V}$ of the matrix $\mathbf{HK}$, so that $\mathbf{HK} = \mathbf{V}\Lambda\mathbf{V}^T$ where Λ is a diagonal matrix composed of the eigenvalues of $\mathbf{HK}$. The projections of $\delta\hat{\mathbf{y}}^a$ onto the eigenvector $\mathbf{V}$ is given by $\mathbf{V}^T\delta\hat{\mathbf{y}}^a = \mathbf{V}^T\mathbf{V}\Lambda\mathbf{V}^T\delta\mathbf{y}^o + \mathbf{V}^T\mathbf{V}(\mathbf{I}_p - \Lambda)\mathbf{V}^T\delta\mathbf{y}^b$, which can be further written as

$$\delta\vec{\hat{\mathbf{y}}}^a = \Lambda\delta\vec{\mathbf{y}}^o + (\mathbf{I}_p - \Lambda)\delta\vec{\mathbf{y}}^b \quad (10)$$

$\delta\vec{\hat{\mathbf{y}}}^a$, $\delta\vec{\mathbf{y}}^o$ and $\delta\vec{\mathbf{y}}^b$ are analysis, observation, and background error in the eigenvector space $\mathbf{V}$ respectively, and are the projections of $\delta\hat{\mathbf{y}}^a$, $\delta\mathbf{y}^o$ and $\delta\mathbf{y}^b$ on the eigenvector $\mathbf{V}$ space. When these vectors are projected on a particular eigenvector $\mathbf{V}_i$ with corresponding eigenvalue equal to λ_i, the above equation can be written as,

For Peer Review

$$\delta\vec{\hat{\mathbf{y}}}_i^a = \lambda_i \delta\vec{\mathbf{y}}_i^o + (1-\lambda_i)\delta\vec{\mathbf{y}}_i^b \tag{11}$$

Therefore, in the eigenvector $\mathbf{V}_i$ space, the analysis sensitivity with respect to the observation is λ_i, and with respect to the background is (1-λ_i). As shown in Cardinali et al. (2004), they are complementary with diagonal observation error covariance.

Schematically, all the elements except λ_i in equation (11) are shown in Figure 1. In the following, we will show how to represent λ_i as a function of the angle α, and to interpret λ_i with the observation error $\delta\vec{\mathbf{y}}_i^o$ and the analysis error $\delta\vec{\hat{\mathbf{y}}}_i^a$. As shown in Figure 1, the observation error ($\delta\vec{\mathbf{y}}_i^o$) and the background error ($\delta\vec{\mathbf{y}}_i^b$) in the eigenvector $\mathbf{V}_i$ space are perpendicular because the background error and observation error are assumed to be uncorrelated, which means that the inner product between $\delta\vec{\mathbf{y}}_i^o$ and $\delta\vec{\mathbf{y}}_i^b$ is 0. The analysis error ($\delta\vec{\hat{\mathbf{y}}}_i^a$) is also perpendicular to the line connecting the observation and the background, reflecting that the analysis is the linear combination of background and observations closer to the truth (Desroziers et al., 2005). With these two relationships, the projection of $\delta\vec{\mathbf{y}}_i^o$ on $\delta\vec{\hat{\mathbf{y}}}_i^a$ is,

$$\begin{aligned} &\delta\vec{\hat{\mathbf{y}}}_i^a \cdot \delta\vec{\mathbf{y}}_i^o = \lambda_i \delta\vec{\mathbf{y}}_i^o \cdot \delta\vec{\mathbf{y}}_i^o \Rightarrow \\ &\left\|\delta\vec{\hat{\mathbf{y}}}_i^a\right\|\left\|\delta\vec{\mathbf{y}}_i^o\right\|\cos(90^\circ-\alpha) = \lambda_i \left\|\delta\vec{\mathbf{y}}_i^o\right\|^2 \end{aligned} \tag{12}$$

Since $\sin(\alpha) = \left\|\delta\vec{\hat{\mathbf{y}}}_i^a\right\| / \left\|\delta\vec{\mathbf{y}}_i^o\right\|$, and $\lambda_i = \left\|\delta\vec{\hat{\mathbf{y}}}_i^a\right\|\left\|\delta\vec{\mathbf{y}}_i^o\right\|\cos(90^\circ-\alpha) / \left\|\delta\vec{\mathbf{y}}_i^o\right\|^2$ based on above equation, then $\lambda_i = \sin^2(\alpha)$ and (1-λ_i) $= \cos^2(\alpha)$. This indicates that the smaller the angle α, the smaller the analysis sensitivity with respect to the observations and the larger the analysis sensitivity to the background. This geometrical representation is

For Peer Review

consistent with equation (6) showing that analysis sensitivity per observation increases with the analysis error and decreases with the observation error.

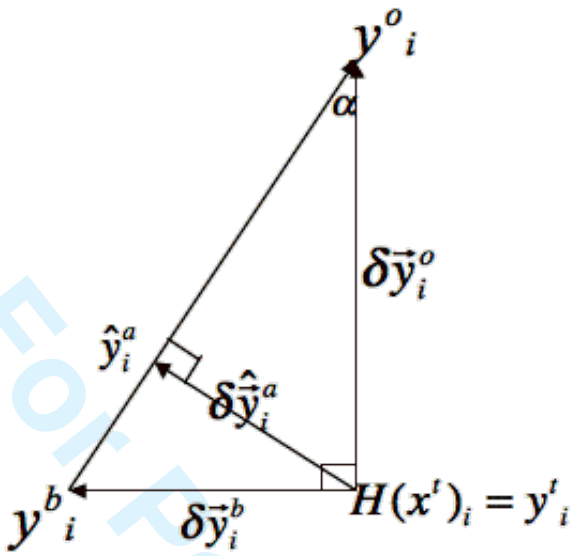

Figure 1 Geometrical representation of the vector elements in equation (11) (see text). The analysis sensitivity with respect to the observations is $\sin^2\alpha$ (adapted from Desroziers et al., 2005).

4. Validation of the self-sensitivity calculation method in EnKF and cross validation experiments with the Lorenz 40-variable model

Cardinali et al. (2004) showed that the change in the analysis $\hat{y}^a_i$ obtained by leaving out the i^{th} observation could be calculated from the self-sensitivity S^o_{ii}, y^o_i and $\hat{y}^a_i$ without calculating $\hat{y}^{a(-i)}_i$ (the estimate of $\hat{y}^a_i$ obtained by leaving out the i^{th} observation), and that the same was true for the calculation of Cross Validation (CV) score (Wahba, 1990, theorem 4.2.1), which is traditionally obtained from leaving out each observation in turn and is defined as $\sum_{i=1}^{m}(y^o_i - \hat{y}^{a(-i)}_i)^2$, m is the total observations.

Therefore, to verify the self-sensitivity calculation method in EnKF (Equation (5)), we will compare $y_i^o - \hat{y}_i^{a(-i)}$ and CV score based on the actual computation of $\hat{y}_i^{a(-i)}$ to those from self-sensitivity following equations (2.9) and (2.10) in Cardinali et al. (2004):

$$\hat{y}_i^a - \hat{y}_i^{a(-i)} = \frac{S_{ii}^o}{(1 - S_{ii}^o)}(y_i^o - \hat{y}_i^a) \tag{13}$$

$$\sum_{i=1}^{m}(y_i^o - \hat{y}_i^{a(-i)})^2 = \sum_{i=1}^{m}\frac{(y_i^o - \hat{y}_i^a)^2}{(1 - S_{ii}^o)^2} \tag{14}$$

With a correct estimation of the self-sensitivity, the left and the right hand sides of equations (13) and (14) should be equal. Deleting each observation in turn is computationally formidable in a realistic NWP data assimilation system, so we use the Lorenz-40 variable for this purpose. It is important to note that the left hand side of Equation (13) estimates the changes that each observation introduces on the analysis. We expect that the analysis change $\hat{y}_i^a - \hat{y}_i^{a(-i)}$ with and without the i^{th} observation will be abnormally large in data sparse regions, or when the atmosphere is unusually sensitive to small perturbations (in the presence of a bifurcation), or when the observation errors are very large. By contrast, we expect the analysis changes to be small in data rich regions. In this section, we will use this characteristic to detect an observation that changes substantially the analysis in a uniform observation coverage scenario without carrying out the denial experiment.

4.1 Lorenz-40 variable model and experimental setup

The Lorenz 40-variable model is governed by the following equation:

For Peer Review

$$\frac{d}{dt}x_j = (x_{j+1} - x_{j-2})x_{j-1} - x_j + F \qquad (15)$$

The variables (x_j, j=1…J) represent a "meteorological" variable on a "latitude circle" with periodic boundary conditions. As in Lorenz and Emanuel (1998), J is chosen to be 40. The time step is 0.05, which corresponds to a 6-hour integration interval. F is the external forcing, which is 8 for the nature run, and 7.6 for the forecast, allowing for some model error in the system. Observations are simulated by adding to the nature run Gaussian random perturbations with standard deviation equal to 0.2.

The data assimilation scheme we use is the Local Ensemble Transform Kalman Filter (LETKF), which is one type of EnKF specifically efficient for parallel computing (see Hunt et al. (2007) for a detailed description of this method). Since F has different values in the nature run and forecast, multiplicative covariance inflation (Anderson and Anderson, 1999) has been applied to account for the model error in addition to the sampling errors. The covariance inflation factor is fixed to be 1.3 in this study, which means that background error covariance $\mathbf{P}^b$ is multiplied by 1.3 during data assimilation. In verifying self-sensitivity calculation method, we use 40 ensemble members, and assume full observation coverage. The analysis sensitivity S_{ii}^o is calculated after each analysis cycle based on equation (6). After full observation data assimilation, each observation is left out in turn to get $\hat{y}_i^{a(-i)}$ using the same background forecasts. To experimentally examine the relationship among analysis sensitivity per observation, observation coverage, and analysis accuracy, we carry out several uniform observation coverage scenarios, namely, 20, 25, 30, 35 and 40 observations. Analysis accuracy is measured by Root Mean Square (RMS) error, which is defined as the RMS difference

For Peer Review

between analysis mean value and the nature run. In order to show that the square of the analysis value change based on the right hand of equation (13) could detect unusual observations, we assign to the observation at the 11th point random errors 4 times larger than to the other observations as in Liu and Kalnay (2008). Since the observation error at the 11th point is much larger than the other points, the square of the analysis value change would be larger than at the other points. For statistic significance of the results, we run each experiment for 1000 analysis cycles, and calculate a time average over the last 500 analysis cycles.

4.2 Results

Comparison between $\hat{y}_i^a - \hat{y}_i^{a(-i)}$ and $\frac{S_{ii}^o}{(1-S_{ii}^o)}(y_i^o - \hat{y}_i^a)$ at a single analysis time (top panel in Figure 2) shows that they have the same value at every grid point, confirming the validity of equation (13). This is also true for the comparison between the cross validation score based on deleting each observation in turn (plus signs in the bottom panel of Figure 2) and that from the self-sensitivity (open circles in the bottom panel of Figure 2). These comparisons prove that the calculation of the self-sensitivity based on equation (6) in EnKF is valid, and that a complete cross-validation that would be unfeasible with the standard approach, can be computed within the ensemble data assimilation cycle based on self-sensitivity. Further experiments with different observation coverage support this conclusion.

Figure 3 shows that self-sensitivity increases with the analysis RMS error, which is consistent with the geometrical interpretation in section 3. Since analysis error is anti-correlated with observation coverage, so is self-sensitivity (Figure 3). The analysis

For Peer Review

sensitivity per observation becomes larger when the observation coverage becomes sparser. The analysis sensitivity per observation is about 0.16 when all the grid points are observed, which indicates that 16% of the information in the analysis comes from the observation at each location. Since the analysis sensitivity with respect to the background is complementary to the analysis sensitivity with respect to the observation (section 3), 84% information of the analysis comes from the background forecast. When only half grid points have observations, the analysis self-sensitivity is about 0.32, which indicates that deletion of one observation in dense observation coverage will do less harm to the analysis system than deletion of one observation in a sparse case. This is consistent with field experiments (e.g., Kelly et al., 2007).

The time-average of the squared analysis value change ($(\hat{y}_i^a - \hat{y}_i^{a(-i)})^2$) based on the right hand side of equation (13) shows the mean squared change at the 11^{th} point, which has 4 times larger random error than the other points, is abnormally large. This confirms that the squared analysis value change based on analysis sensitivity can be used to detect abnormal observations very efficiently at the analysis time, without performing data denial experiments. In a real NWP scenario, in which the observation coverage is not uniform, an abnormal behavior of the observations based on the change of the analysis value may come from the non-uniform observation coverage: the value should be larger in data sparse areas. However, since the calculation of the absolute analysis value change based on equation (13) is very simple and requires little computational time, it could be used as a sophisticated observation quality check.

For Peer Review

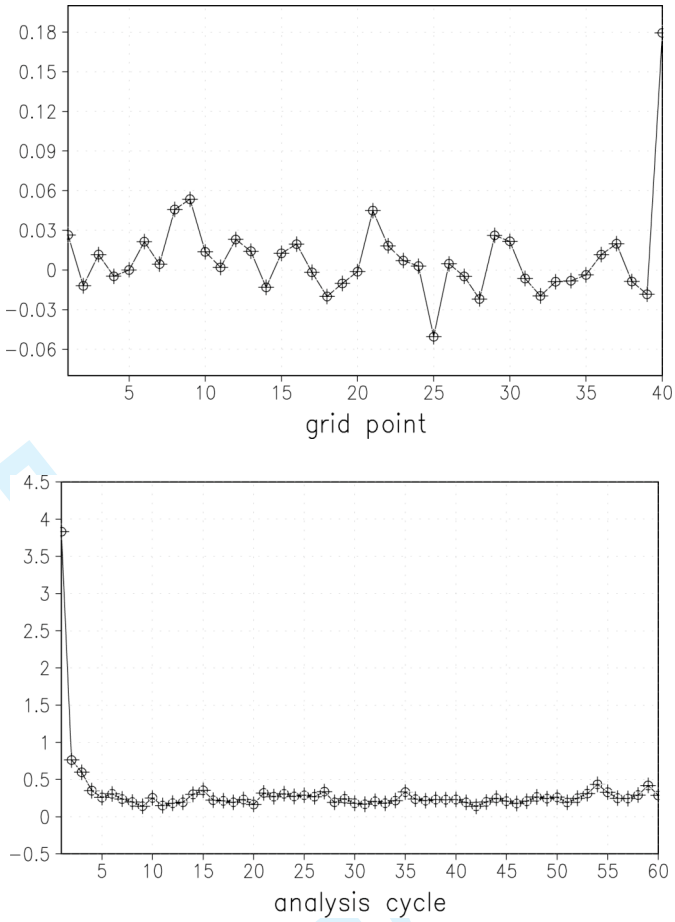

Figure 2 Top panel: $\hat{y}_i^a - \hat{y}_i^{a(-i)}$ (plus sign) and $\frac{S_{ii}^o}{(1-S_{ii}^o)} r_i$ (open circles) comparison at one analysis time as function of grid point. Bottom panel: comparison of CV score calculated from $\sum_{i=1}^{m} (y_i^o - \hat{y}_i^{a(-i)})^2$ (plus sign) and that from $\sum_{i=1}^{m} \frac{(y_i^o - \hat{y}_i^a)^2}{(1-S_{ii}^o)^2}$ (open circles) in the first 60 analysis cycles.

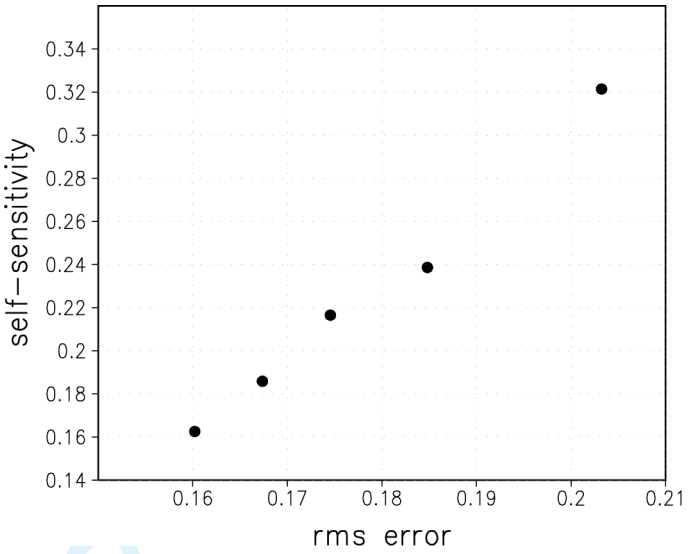

Figure 3 Scatter plot of the time averaged analysis sensitivity per observation (y-axis) and the analysis RMS error (x-axis) (from bottom to top, the points correspond to 40 observations, 35 observations, 30 observation, 25 observation and 20 observations).

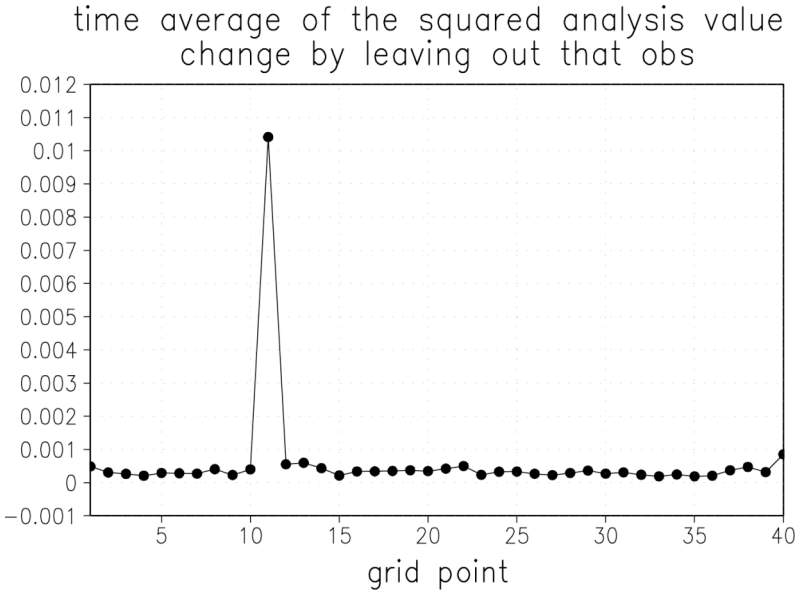

Figure 4 Time average of the squared analysis value change (equation (13)) by leaving out each observation in turn. The observation error at the 11th point is four times larger than the errors of the other observations.

5. Consistency between information content and the observation impact obtained from data denial experiments

Equation (13) indicates that the deletion of an observation with larger self-sensitivity will result in larger change in the analysis value compared to the deletion of

other observations. Assuming that the correction to the analysis by that observation is to make analysis better, which is true statistically when error statistics used in data assimilation are correct, the deletion of that observation will result in a worse analysis than the deletion of other observations. Equation (13) is only valid when one observation is left out. However, in most NWP cases, we need to examine the impact of a subset of observations on analysis, which is usually done by data denial experiments. In this section, we will explore whether the trace of self-sensitivity of a subset of observations, which is referred to as *information content*, can qualitatively show the actual observation impact from data denial experiments.

5.1 Experimental setup

We use the Simplified Parameterizations primitivE Equation DYnamics (SPEEDY, Molteni, 2003) model, which is a global atmospheric model with 96x48 grid points in horizontal and 7 vertical levels. We follow a "perfect model" Observing System Simulation Experiments (OSSEs, e.g., Lord et al. 1997) setup, in which the simulated truth is generated with the same atmospheric model as the one used in data assimilation (identical twin experiment). Observations are simulated by adding Gaussian random noise to the truth. The observation error standard deviations assumed for winds and specific humidity is about 30% of their natural variability, shown in Figure 5. The specific humidity is only observed in the lowest five vertical levels, below 300hPa. Since temperature variability does not change much with vertical levels, we assume the observation error standard deviation is 0.8K in all vertical levels. The error standard deviation for surface pressure is 1.0hPa. In such an experimental setup, the observation error statistics is fairly accurate, and so is the analysis error statistics estimated in each

For Peer Review

analysis cycle. We carry out 1.5-month data assimilation cycles using the LETKF data assimilation scheme. The results shown in this section are averaged over the last one-month.

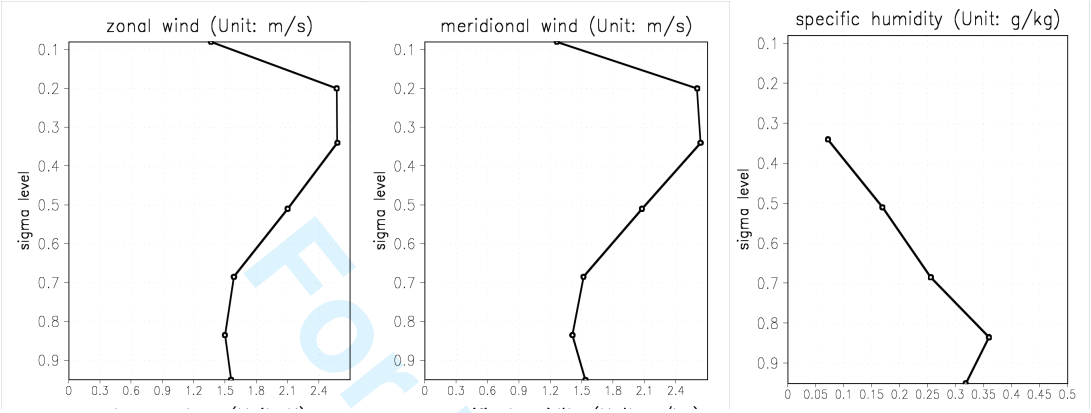

Figure 5 The observation error standard deviation for zonal wind (Unit: m/s, left panel), meridional wind (Unit: m/s, middle panel) and specific humidity (Unit: g/kg, right panel).

In the data denial experimental setup, the control experiment (called *all-obs*) has full observation coverage (Figure 6). In each observation location, circles and crosses, all the prognostic variables (u, v, T, q, p_s) are observed in every vertical level. In the data denial experiments, the denied variable is only observed at the "rawinsonde" locations (closed circles in Figure 6). For instance, in the *no-u* sensitivity experiment, zonal wind observations are still observed at the rawinsonde locations but not at the locations marked with plus signs. We compare the *information content* of zonal wind observations over the locations with plus signs with the actual observation impact obtained as the analysis error difference between *no-u* and *all-obs* experiment. Again, the information content is the summation of self-sensitivity, which is calculated from equation (6) based on ensemble analyses of the control run. We also do a similar comparison for *no-q* sensitivity experiment. Ideally, the area with larger information content will correspond to the area

For Peer Review

with larger error differences between the much more expensive sensitivity experiment and the control run.

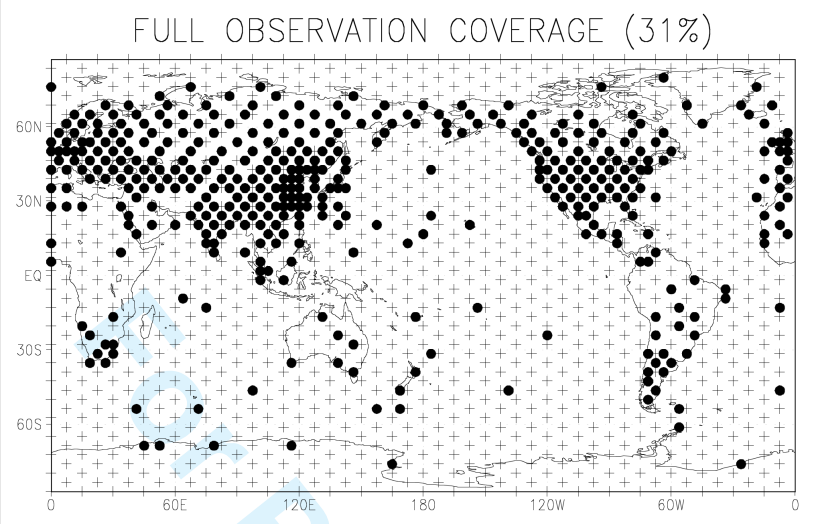

Figure 6 Full observation distribution (closed dots: rawinsonde observation network; plus signs: dense observation network), every observation location is at the grid point.

5.2 Results

Figure 7 shows zonal mean zonal wind analysis RMS error difference (contours) between *no-u* and *all-obs* and the information content (shaded) of zonal wind observations. Here, the information content is the trace of zonal wind self-sensitivity at the locations with plus signs in each latitude circle (Figure 6), which reflects the information extracted from these zonal wind observations at that latitude. Quantitatively, the analysis RMS error difference (contour) between *no-u* and *all-obs* experiment is largest over the tropics, and is smallest over the mid-latitude Northern Hemisphere (NH). Qualitatively, the information content (shaded area) agrees with this RMS error difference, showing the largest values over the tropics and smallest values in the mid-latitude NH. Interestingly, the zonal wind observations have relatively small impact over the mid-latitude Southern Hemisphere (SH), even though the rawinsonde coverage is

For Peer Review

sparse over that region. This is because in the *no-u* experiment the mass fields, such as temperature and surface pressure, update the winds analysis in the mid-latitude SH through the error covariance between these variables. The information content basically reflects this feature, also showing relatively small values over that region.

Figure 8 shows time averaged zonal wind self-sensitivity (filled grid points) at observation locations with plus signs (Figure 6) and zonal wind RMS error difference between *no-u* and control run at the sixth model level. It shows that self-sensitivity has a larger value between 30ºS and 30ºN, and so does RMS error difference. However, we should not over interpret this result. For any two single points, the relative magnitude of self-sensitivity may not reflect the relative magnitude of RMS error difference between *no-u* and control run due to sampling errors. Self-sensitivity can only qualitatively show the observation impact over some spatial domain. Since the summation of self-sensitivity and the sensitivity of the analysis with respect to the background at the same observation location are equal to 1, Figure 8 indicates that analysis state extracts most of the information from background forecasts, which is consistent with Cardinali et al. (2004).

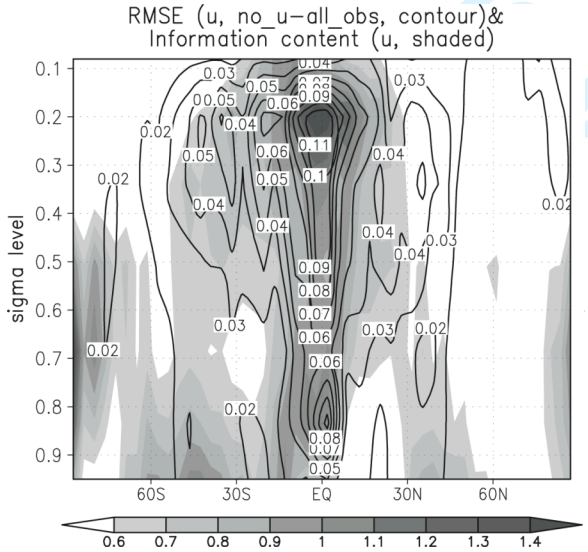

Figure 7 Zonal wind RMS error difference (contour, unit: m/s) between sensitivity experiment and control experiment, and zonal wind information content (shaded) over observation locations with plus sign.

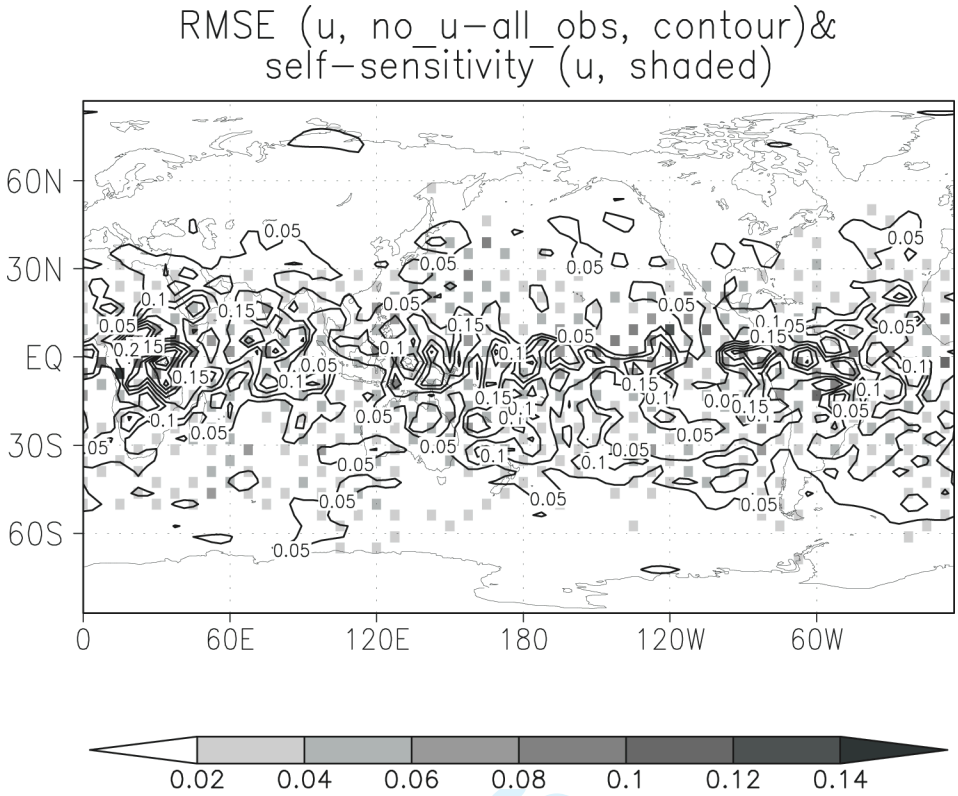

Figure 8 Time averaged zonal wind RMS error difference (contour; unit: m/s) between *no-u* and control experiment at the sixth model level and self-sensitivity (filled grid point) of zonal wind observations at locations with plus signs in Figure 6 at the sixth model level.

The highly spatial temporal variability and nonlinear physical processes related with humidity make humidity observation impact study a very challenging problem (e.g., Langland and Baker, 2004). In spite of these challenges, the spatial distribution of specific humidity information content is consistent with the specific humidity RMS error difference between *no-q* and *all-obs* experiment (left panel in Figure 9). It is important to note that the information content of specific humidity observations qualitatively reflects not only the impact on the humidity analysis field, but also the impact on the other dynamical variables, such as zonal wind (right panel in Figure 9). This originates from

multivariate characteristics in *all-obs* experiment, in which specific humidity observations linearly affect winds through the covariance, and this effect is maximized in the tropical upper troposphere (right panel in Figure 9). This large impact of humidity observations on wind analyses over high tropical levels is consistent with the multivariate assimilation of AIRS humidity retrievals in a low resolution NCEP Global Forecast System (Liu, 2007).

The horizontal distribution of specific humidity self-sensitivity (Figure 10) is also qualitatively consistent with the analysis RMS error difference between *no-q* and control run for both specific humidity and zonal wind. Interestingly, information content and self-sensitivity of specific humidity observations (Figure 9 and Figure 10) are larger than those of zonal wind observations (Figure 7 and Figure 8). This means specific humidity analyses extract more information from humidity observations than zonal wind analyses extract from zonal wind observations. However, this does not mean that assimilating specific humidity observations would reduce more error than assimilating zonal wind observations. This is because specific humidity and zonal wind have different dynamical roles in the forecast system. The large-scale interaction between zonal wind and the other dynamical variables during forecast may make zonal wind observations more important to reduce the overall analysis RMS error. Therefore, information content may not be applicable to examine the relative impact of observations belonging to different dynamical variable types on a data assimilation and forecasting system for which forecast sensitivity to observations may be a more appropriate measure (Langland and Baker, 2004, Liu and Kalnay, 2008). Nevertheless, the qualitative consistency between information content and the actual observation impact from data denial experiments

For Peer Review

suggests that we can examine the relative impact of the same dynamical variable type observations in different locations using information content without actually carrying out much more expensive data denial experiments.

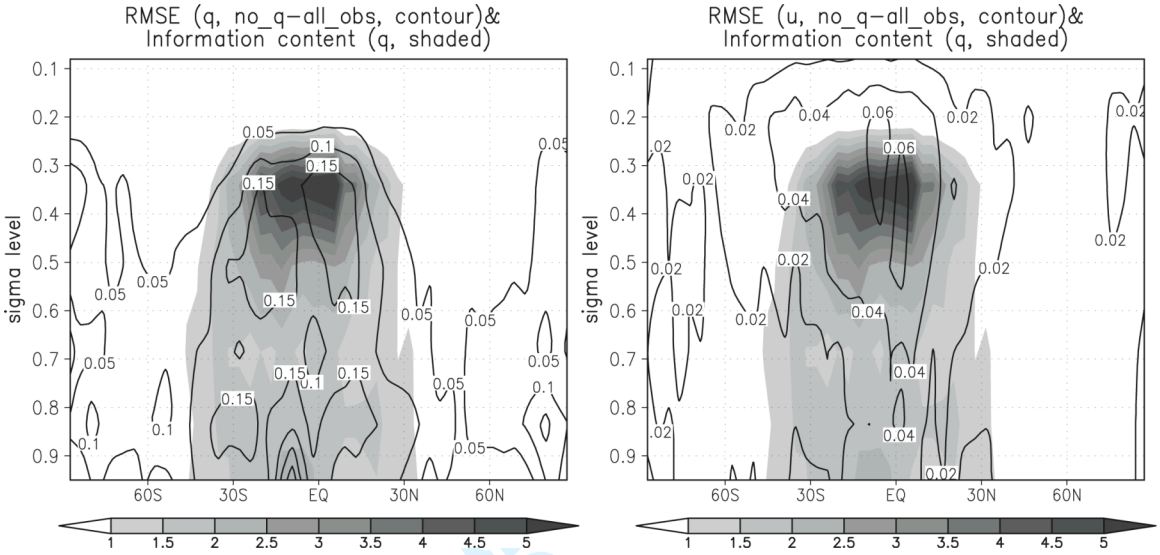

Figure 9 RMS error difference (contour) between *no-q* and *all-obs* experiment and specific humidity information content (shaded) (Left panel: specific humidity RMS error difference (Unit: 10^{-1}g/kg); right panel: zonal wind RMS error difference (Unit: m/s)).

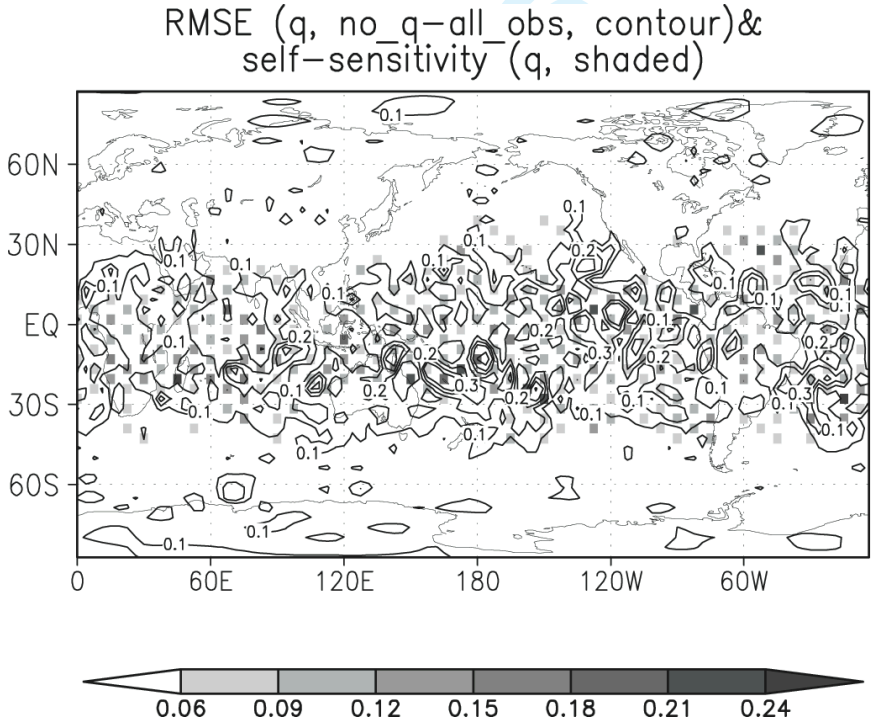

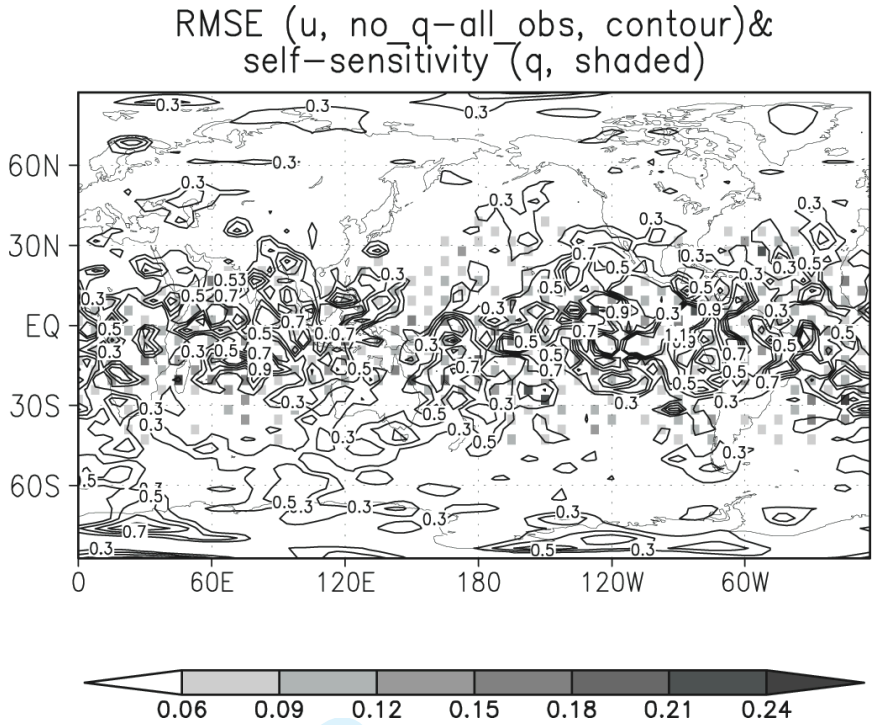

Figure 10 The time averaged RMS error difference (contour) between *no-q* and *all-obs* experiment and the self-sensitivity (filled grid point) of specific humidity observations at locations with plus signs (Figure 6) at the fourth model level (Top panel: specific humidity RMS error difference (Unit: 10^{-1}g/kg); bottom panel: zonal wind RMS error difference (Unit: 10^{-1}m/s)).

6. *Conclusions and discussion*

The influence matrix reflects the regression fit of the analysis to observations, and self-sensitivity (diagonal value of influence matrix) gives a measure of the analysis sensitivity to observations. Information content, defined as the trace of the self-sensitivity, reflects the information extracted from a subset of observations during data assimilation. These measures show the analysis sensitivity to observations, and can further show the relative impact of the same type observations on the performance of the analysis system when the statistics used in the data assimilation reflects the true uncertainty of each factor.

For Review

Following the work of Cardinali et al. (2004) within the ECMWF 4D-Var system, we showed how to calculate self-sensitivity and cross sensitivity (off-diagonal elements of influence matrix) in the EnKF framework. Based on ensemble analyses generated in each analysis cycle, the calculation of self-sensitivity and cross-sensitivity in EnKF only needs the application of the observation operator on each analysis ensemble member and performing scalar product calculations (equations (6) and (7) in section 2). By comparing cross-validation (CV) scores calculated from leaving out each observation in turn and that is based on self-sensitivity, we verified the self-sensitivity calculation and cross-validation method in EnKF with Lorenz-40 variable model. Unlike the self-sensitivity calculation in 4D-Var (Cardinali et al., 2004), the self-sensitivity calculated in EnKF satisfies the theoretical value limits (between 0 and 1) when the observation errors are not correlated. In agreement with the geometrical interpretation, we showed experimentally that self-sensitivity is proportional to the analysis errors and anti-correlated with the observation coverage when the error statistics used in the data assimilation are fairly accurate.

The squared analysis value change based on analysis sensitivity can be used to detect observations that produce an unusually large impact on the analysis. This large impact could be due to large errors in the observations, to the observations being isolated, or to the atmosphere having a high regional sensitivity to perturbations leading to large forecast error growth. It would be unfeasible to carry out such computations in its original formulation even for a model with a moderate number of degrees of freedom. The computation of the squared analysis value change from leaving out each observation in turn becomes efficient when using analysis sensitivity in an EnKF but not in the

For Peer Review

variational formulation because in EnKF no approximations are made in calculating the sensitivities. We showed that the ability to identify observations that produce unusually large changes in the analysis can be efficiently used to identify faulty observations during the analysis cycle, similar to the forecast sensitivity method of Langland and Baker (2004), Zhu and Gelaro (2008) and Liu and Kalnay (2008).

In an idealized experimental setup, the comparison between information content and the actual observation impact given by data denial experiments shows qualitative agreement. This implies that the spatial distribution of information content can be utilized in examining the relative importance of the same dynamical variable type observations without actually carrying out much more expensive data denial experiments. However, information content may not reflect the relative importance of observations from different dynamical variable types since the relative importance of different dynamical variable type of observations is also related with the dynamical role they played in the forecast system. In the future, we will use self-sensitivity and information content to estimate the importance of the assimilated observations in a more realistic data assimilation system.

For Peer Review

Acknowledgements

We are grateful to weather Chaos group in Maryland for suggestions and discussions, and an anonymous reviewer whose valuable suggestions greatly improved the manuscript. This work has been supported by NASA grants NNG06GB77G, NNX07AM97G, NNX08AD40G, and DOE grants DEFG0207ER64437.

References

Anderson, J. L. (2001), An ensemble adjustment Kalman filter for data assimilation. *Mon. Wea. Rev.*, **129**, 2884-2903.

Anderson, J. L. and S. L. Anderson (1999), A Monte Carlo implementation of the nonlinear filtering problem to produce ensemble assimilations and forecasts. *Mon. Wea. Rev.,* **127,** 2741–2758.

Bishop, C. H., B. Etherton, and S. J. Majumdar (2001), Adaptive sampling with the ensemble transform Kalman filter. Part I: Theoretical aspects. *Mon. Wea. Rev.,* **129***,* 420-436.

Cardinali, C., S. Pezzulli, and E. Andersson (2004), Influence-matrix diagnostic of a data assimilation system. *Quart. J. Roy. Meteor. Soc.* **130***,* 2767-2786

Desroziers, G., L. Berre, B. Chapnik, and P. Poli (2005), Diagnosis of observation, background and analysis error statistics in observation space. *Quart. J. Roy. Meteor. Soc.,* **131***,* 3385-3396.

Evensen, G. (1994), Sequential data assimilation with a nonlinear quasi-geostrophic model using Monte Carlo methods to forecast error statistics. *J. Geophys. Res.,* **99** (C5), 10 143-10 162.

Houtekamer, P. L. and H. L. Mitchell (2001), A sequential Ensemble Kalman Filter for atmospheric data assimilation. *Mon. Wea. Rev.*, **129**, 123-137.

Hunt, B. R., E. J., Kostelich, and I., Szunyogh (2007), Efficient Data Assimilation for Spatiotemporal Chaos: a Local Ensemble Transform Kalman Filter. *Physics D.*, **230**, 112-126.

For Peer Review

Kelly, G., J-N Thepaut, R. Buizza and C. Cardinali (2007), The value of targeted observations part I : the value of observations taken over the oceans. ECMWF's status and plans. ECMWF Tech. Memo., 511, pp27.

Langland, R. H. and Baker, N. L., 2004: Estimation of observation impact using the NRL atmospheric variational data assimilation adjoint system. *Tellus*, **56a**, 189-201.

Liu, J. (2007), Applications of the LETKF to adaptive observations, analysis sensitivity, observation impact, and assimilation of Moisture. Ph. D thesis, University of Maryland.

Liu, J. and E. Kalnay, 2008: Estimating observation impact study without adjoint model in an ensemble Kalman filter. *Quart. J. Roy. Meteor. Soc,* **134***,* 1327-1335.

Lord, S. J., E. Kalnay, R. Daley, G. D. Emmit, and R. Atlas: 1997, Using OSSEs in the design of the future generation of integrated observing system. 1st Symposium on Integrated Observation Systems, AMS

Lorenz, E. N. and K. A. Emanuel (1998), Optimal sites for supplementary observations: Simulation with a small model. *J. Atmos. Sci.,* **55***,* 399-414.

Molteni, F., (2003), Atmospheric simulations using a GCM with simplified physical parametrizations. I: Model climatology and variability in multi-decadal experiments. *Climate Dyn.*, **20**, 175-191.

Ott, E., B. R. Hunt, I. Szunyogh, A. V. Zimin, E. J. Kostelich, M. Corazza, E. Kalnay, D. J. Patil, and J. A. Yorke (2004), A Local Ensemble Kalman Filter for Atmospheric Data Assimilation. *Tellus*, **56A**, 415-428

Rabier, F., N. Fourrie, D. Chafai and P. Prunet (2002), Channel selection method for Infrared Atmospheric Sounding Interferometer radiances. *Quart. J. Roy. Meteor. Soc.* **128**, 1011-1027.

For Peer Review

Wahba, G. (1990), *Spline models for observational data.* CMMS-NSF, Regional conference series in applied mathematics, volume 59. Society for Industrial and Applied Mathematics.

Whitaker, J. S., and T. M. Hamill (2002), Ensemble data assimilation without perturbed observations. *Mon. Wea. Rev.* **130**, 1913-1924.

Zhu, Y. and Gelaro, R., 2008: Observation sensitivity calculations using the adjoint of the Gridpoint Statistical Interpolation (GSI) analysis system. *Mon. Wea. Rev.* **136**, 335-351.

For Peer Review